Neutron Spectroscopy, IR, Raman and *Ab Initio* Study of L-Proline

by A. Pawlukojć[1,2*], J. Leciejewicz[2], I. Natkaniec[1,3] and J. Nowicka-Scheibe[4]

[1] *Joint Institute for Nuclear Research, 141980 Dubna, Russia*
[2] *Institute of Nuclear Chemistry and Technology, 03 195 Warszawa, Poland*
[3] *H. Niewodniczański Institute of Nuclear Physics, Krakow, Poland*
[4] *Institute of Fundamental Chemistry, Technical University, Szczecin, Poland*

Inelastic incoherent neutron scattering spectra (IINS) were obtained for normal and deuterated L-proline. Raman and infrared spectra were also recorded. Geometries were optimized for the zwitterion form using *ab initio* Hartree-Fock (HF) level with 6-31G*, 6-311G** and 6-311++G** basis sets. Force fields and normal modes were calculated and used as basis for an assignment of the spectral features. The theoretical frequencies of normal and d_2 – L-proline were compared with IINS spectra.

Key words: L-proline, inelastic neutron scattering, infrared, Raman, *ab initio* calculations

L-proline (pyrrolidine-2-carboxylic acid) is an amino acid containing a pyrrolidine five membered ring. Due to its size, the molecule may introduce significant perturbations in the molecular framework of many natural proteins – hence interest in its structure and properties. An X-ray diffraction study revealed that in the crystals the molecule of L-proline exists in the zwitterionic form and both hydrogen atoms attached to the pyrrolidine ring nitrogen atom take part in hydrogen bonds responsible for the cohesion of the crystal [1]. The molecule of L-proline with atom numbering scheme is shown in Fig. 1. *Ab initio* assignments of experimental IR and Raman spectra [2] were done at first assuming the non-ionized form of the molecule [3]; later the zwitterion model was used [4].

It has been shown in recent years, that the spectroscopy of incoherently scattered thermal neutrons (IINS) provides important information on the molecular motions in crystals, in particular, on the dynamics of hydrogen bonds in the crystals of amino acids (see for example [5–7]). Since the hydrogen nuclei exhibit large cross section for incoherent scattering of thermal neutrons, the internal modes, in which hydrogen atoms participate, produce IINS spectra of much higher intensity than other modes. Moreover, the substitution of hydrogen by deuterium, which has the incoherent cross section forty times smaller, while the oscillator mass is twice as large, makes it possible to identify uniquely the modes of hydrogen vibrations. Therefore, in addition to the IR and Raman spectra we have measured the IINS spectra of normal

---

* Corresponding author. E-mail: andrzej@nf.jinr.ru

and deuterated L-proline. In all experiments, *ab initio* calculations have been used for the assignment of the relevant modes.
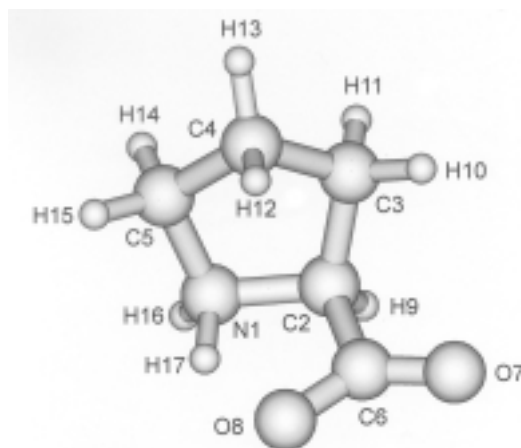

Figure 1. The molecule of L-proline with the atom labelling scheme.

EXPERIMENTAL

A polycrystalline sample of L-proline (Aldrich) was used for experimental data collection. The deuterated sample, in which 98% of acidic protons was substituted by deuterions, was obtained by recrystallization of L-proline from heavy water D_2O. Neutron scattering data were collected at the pulsed reactor IBR-2 in Dubna, using the inverted geometry time-of-flight spectrometer NERA-PR [8]. In the energy transfer range from 5 to 100 meV the relative resolution of this instrument is about 3%. The incident neutron energy was determined by the reactor-sample flight path of 109.05 m and the energy of the scattered neutrons by the pyrolitic graphite analysers (E_f = 4.7 meV) mounted behind a beryllium filter. The spectra were recorded at 22 K and at the room temperature. Time of flight spectra were converted to phonon density of states $G(\omega)$ function and corrected for the background using standard procedures [9]. The $G(\omega)$ *versus* energy transfer curve for the normal L-proline is displayed in Fig. 2; for the deuterated sample – in Fig. 3. These curves will be subsequently called "IINS spectra".

The infrared spectra were recorded on a Perkin-Elmer System 2000 R FTIR/FT-Raman spectrometer with a Diode Pumped Nd:YAG laser (2W). The absorption IR spectra were measured in the range from 400 cm^{-1} to 3600 cm^{-1} and from 100 cm^{-1} to 450 cm^{-1} with intervals of 0.5 cm^{-1} and the resolution of 4 cm^{-1}. These spectra are shown in Figs. 4 and 5. The FT-Raman spectra were recorded using a polycrystalline sample in a glass capillary. The resolution was 4 cm^{-1}, laser power 400mW, Nd:YAG laser wave number 9394.7 cm^{-1}. These spectra are shown in Fig. 6.

Computing details: *Ab initio* calculations for the zwitterion of L-proline were performed at HF level with 6-31G**, 6-311G** and 6-311++G** sets using the program Gaussian 98 [10]. The starting molecular geometry was taken from the X-ray structure [1]. Optimized bond lengths, bond angles and torsional angles of L-proline are listed in Table 1. Among different *ab initio* methods, only DFT and MP2 calculations produced the zwitterionic form. The vibrational frequencies for the normal and deuterated sample of L-proline were calculated using the optimized geometries derived from HF/6-31G**, HF/6-311G** and HF/6-311++G** models of the zwitterionic form. The calculated frequencies were scaled scale factor as recommended for the HF methods [10]. The harmonic force field (second derivative of energy in respect to internal coordinates) and potential energy distribution (PED) were evaluated at HF/6-31G** level using the PC GAMESS version [11] of the GAMESS (US) QC package [12].

Figure 2. Experimental IINS spectrum of normal L-proline recorded at 22 K (bottom). Simulated spectra using the CLIMAX program are shown above.
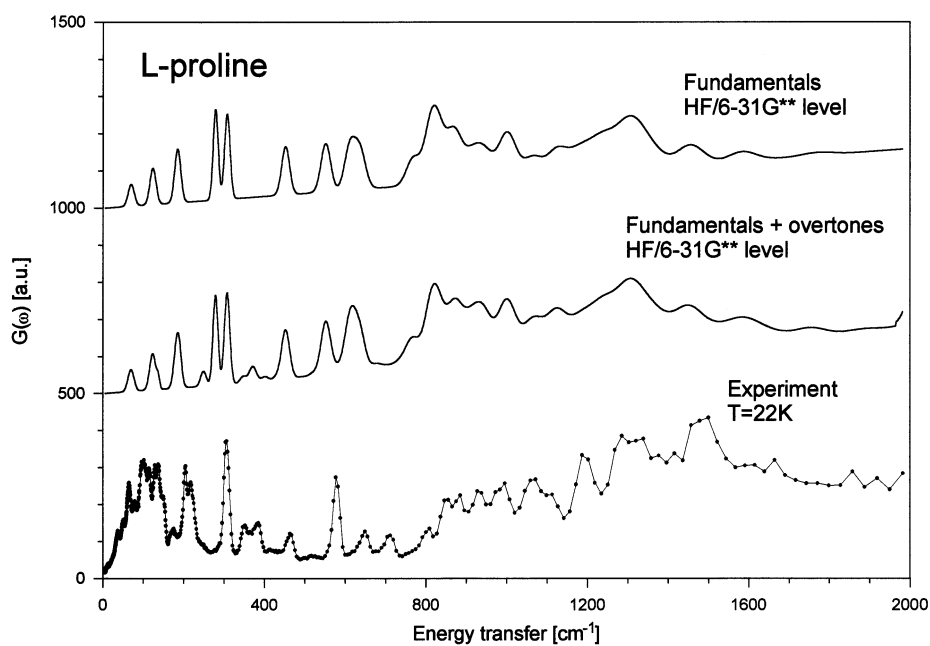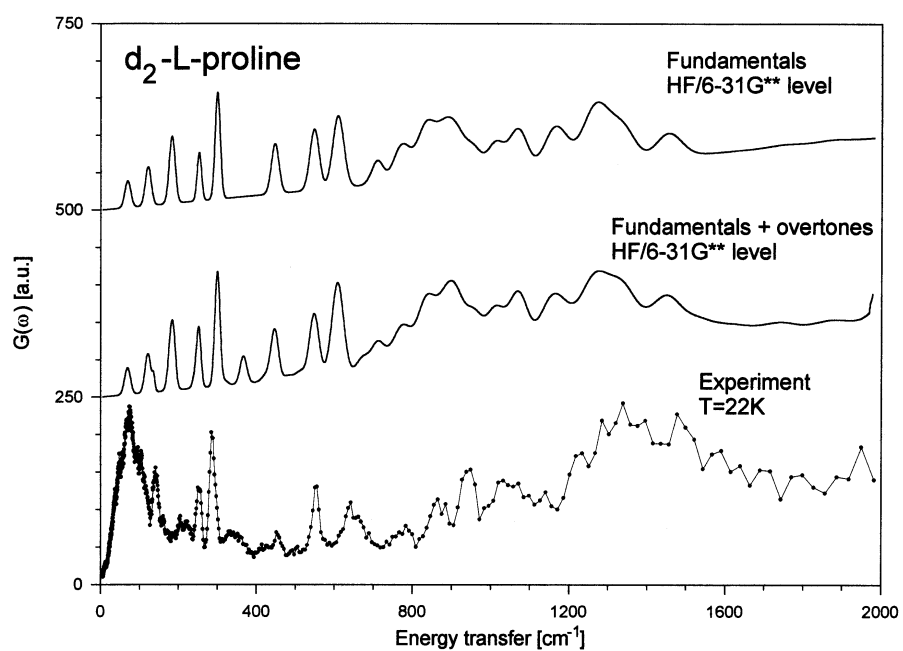

Figure 3. Experimental IINS spectrum of the deuterated L-proline recorded at 22 K (bottom). Simulated spectra using the CLIMAX program are also shown.
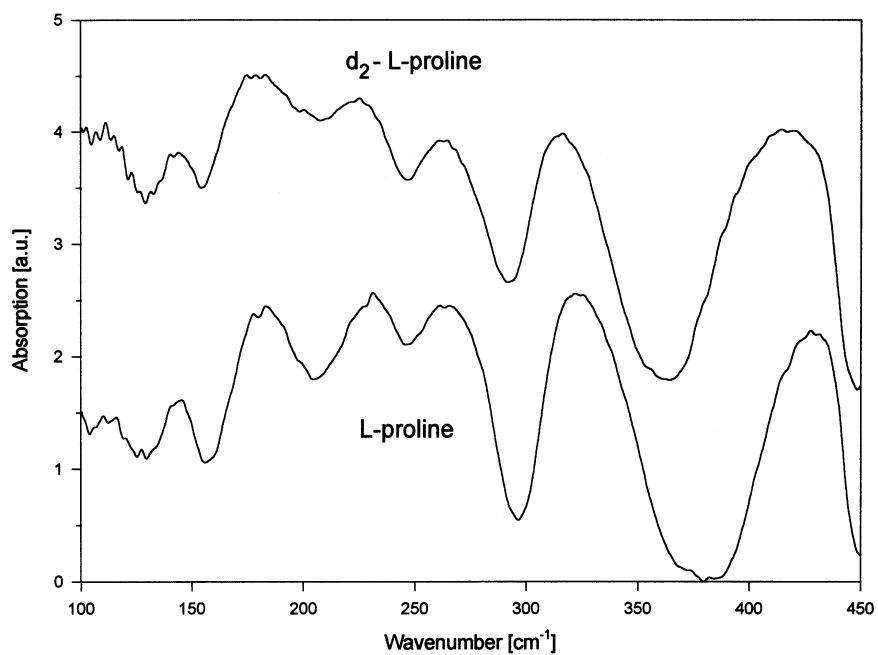
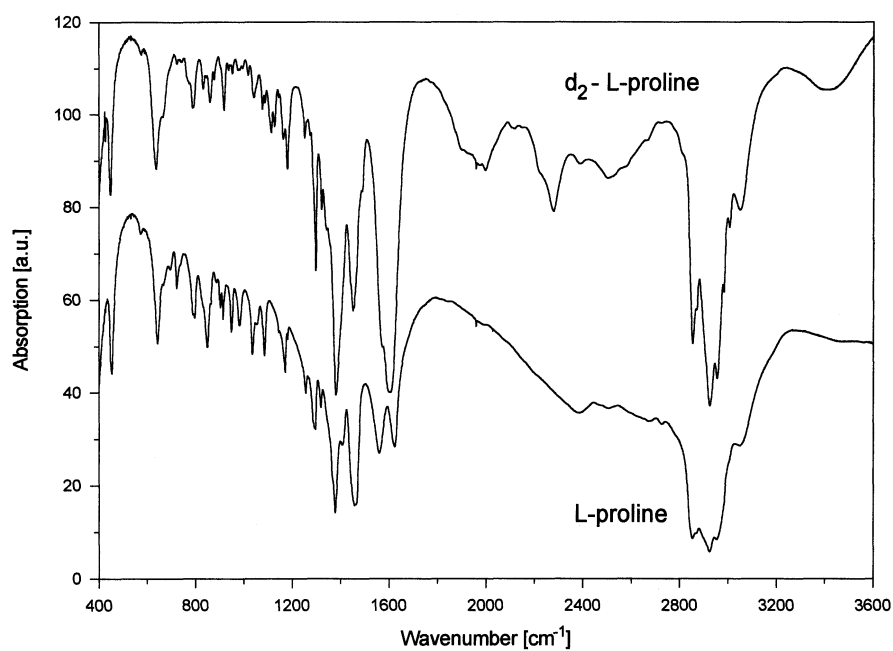**Figure 4.** Infrared spectra of normal and deuterated L-proline in the frequency range from 100 to 450 cm^{-1}.

Figure 5. Infrared spectra of normal and deuterated L-proline in the frequency range from 400 to 3600 cm^{-1}.
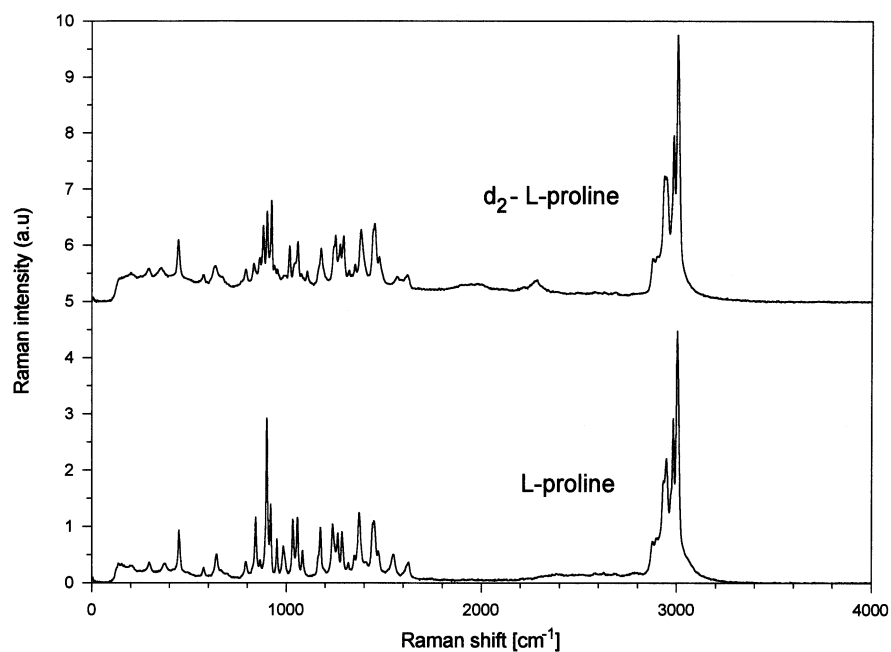
Figure 6. Raman spectra of normal and deuterated L-proline.

Table 1. The structural parameters of L-proline.

Coordinates	Calculated HF/			Experiment
	6-31G**	6-311G**	6-311++G**	X-ray [1]
N1–C2	1.510	1.511	1.512	1.527
C2–C3	1.527	1.527	1.527	1.522
C3–C4	1.532	1.531	1.531	1.538
C4–C5	1.527	1.527	1.527	1.532
C5–N1	1.491	1.491	1.493	1.484
C2–C6	1.568	1.571	1.569	1.527
C6–O7	1.207	1.202	1.205	1.258
C6–O8	1.247	1.241	1.240	1.275
N1–H16	1.00	1.00	1.00	0.998
N1–H17	1.06	1.05	1.04	0.984
N1...O8	2.429	2.373	2.439	2.609
N1–C2–C3	104.7	104.7	104.7	106.2
C2–C3–C4	103.2	103.2	103.2	100.8
C3–C4–C5	103.0	104.2	102.9	103.6
C4–C5–N1	103.7	104.2	103.6	105.3
C5–N1–C2	109.2	109.0	109.2	107.1
N1–C2–C6	104.2	102.0	104.5	106.4
C3–C2–C6	113.1	114.4	113.3	111.5
C2–C6–O7	115.4	115.0	115.1	120.8
C2–C6–O8	112.1	111.0	112.2	119.0
O7–C6–O8	132.5	132.9	132.6	120.2

Table 1 (continuation)

N1–C2–C3–C4	28.2	31.2	28.0	33.6
C2–C3–C4–C5	–40.0	–39.0	–40.2	–41.0
C3–C4–C5–N1	36.3	31.3	36.7	33.6
C4–C5–N1–C2	–19.0	–11.9	–19.6	–12.4
C5–N1–C2–C3	–5.8	–12.1	–5.4	–13.7
C6–C2–C3–C4	–84.7	–79.5	–85.2	–82.0
C6–C2–N1–C5	113.2	107.3	113.9	105.3
O7–C6–C2–C3	–63.3	–56.2	–64.2	–74.0
O7–C6–C2–N1	–176.5	–168.5	–177.5	170.6
O8–C6–C2–C3	115.8	113.5	115.1	108.6
O8–C6–C2–N1	2.6	1.2	1.8	–6.9

The internal coordinates and normal modes are defined in Table 2. The computational results, the experimental IINS, IR and Raman data and their assignments are collected in Table 3. In addition, the IINS spectra were simulated using the CLIMAX program [13] taking the parameters of the NERA-PR experiment. They are compared with the IINS spectra in Figs. 2 and 3. All computations were carried out using an HP-SPP computer at the Joint Institute of Nuclear Research in Dubna.

Table 2. Symmetry coordinates of L-proline.

Coordinate	Description
$S_1 = R_{1,16} + R_{1,17}$	NH_2^+ str. symm.
$S_2 = R_{1,16} - R_{1,17}$	NH_2^+ str. asymm.
$S_3 = R_{3,10} + R_{3,11}$	$C3H_2$ str. symm.
$S_4 = R_{3,10} - R_{3,11}$	$C3H_2$ str. asymm.
$S_5 = R_{4,12} + R_{4,13}$	$C4H_2$ str. symm.
$S_6 = R_{4,12} - R_{4,13}$	$C4H_2$ str. asymm.
$S_7 = R_{5,14} + R_{5,15}$	$C5H_2$ str. symm.
$S_8 = R_{5,14} - R_{5,15}$	$C5H_2$ str. asymm.
$S_9 = R_{2,9}$	C2H str.
$S_{10} = R_{6,7} + R_{6,8}$	COO^- str. symm.
$S_{11} = R_{6,8} - R_{6,8}$	COO^- str. asymm.
$S_{12} = R_{2,6}$	C2C6 str.
$S_{13} = R_{1,2}$	N1C2 str.
$S_{14} = R_{2,3}$	C2C3 str.
$S_{15} = R_{3,4}$	C3C4 str.
$S_{16} = R_{4,5}$	C4C5 str.
$S_{17} = R_{5,1}$	C5N1 str.
$S_{18} = \alpha_{5,1,16} + \alpha_{2,1,16} + \alpha_{5,1,17} + \alpha_{2,1,17}$	NH_2^+ bend.
$S_{19} = \alpha_{5,1,16} - \alpha_{2,1,16} + \alpha_{5,1,17} - \alpha_{2,1,17}$	NH_2^+ wagg.
$S_{20} = \alpha_{5,1,16} - \alpha_{2,1,16} - \alpha_{5,1,17} + \alpha_{2,1,17}$	NH_2^+ twist.
$S_{21} = \alpha_{5,1,16} + \alpha_{2,1,16} - \alpha_{5,1,17} - \alpha_{2,1,17}$	NH_2^+ rock.
$S_{22} = \alpha_{2,3,10} + \alpha_{4,3,10} + \alpha_{2,3,11} + \alpha_{4,3,11}$	$C3H_2$ bend.
$S_{23} = \alpha_{2,3,10} - \alpha_{4,3,10} + \alpha_{2,3,11} - \alpha_{4,3,11}$	$C3H_2$ wagg.
$S_{24} = \alpha_{2,3,10} - \alpha_{4,3,10} - \alpha_{2,3,11} + \alpha_{4,3,11}$	$C3H_2$ twist.
$S_{25} = \alpha_{2,3,10} + \alpha_{4,3,10} - \alpha_{2,3,11} - \alpha_{4,3,11}$	$C3H_2$ rock.
$S_{26} = \alpha_{3,4,12} + \alpha_{5,4,12} + \alpha_{3,4,13} + \alpha_{3,4,13}$	$C4H_2$ bend.
$S_{27} = \alpha_{3,4,12} - \alpha_{5,4,12} + \alpha_{3,4,13} - \alpha_{3,4,13}$	$C4H_2$ wagg.
$S_{28} = \alpha_{3,4,12} - \alpha_{5,4,12} - \alpha_{3,4,13} + \alpha_{3,4,13}$	$C4H_2$ twist.
$S_{29} = \alpha_{3,4,12} + \alpha_{5,4,12} - \alpha_{3,4,13} - \alpha_{3,4,13}$	$C4H_2$ rock.
$S_{30} = \alpha_{4,5,14} + \alpha_{1,5,14} + \alpha_{4,5,15} + \alpha_{1,5,15}$	$C5H_2$ bend.
$S_{31} = \alpha_{4,5,14} - \alpha_{1,5,14} + \alpha_{4,5,15} - \alpha_{1,5,15}$	$C5H_2$ wagg.
$S_{32} = \alpha_{4,5,14} - \alpha_{1,5,14} - \alpha_{4,5,15} + \alpha_{1,5,15}$	$C5H_2$ twist.
$S_{33} = \alpha_{4,5,14} + \alpha_{1,5,14} - \alpha_{4,5,15} - \alpha_{1,5,15}$	$C5H_2$ rock.

Table 2 (continuation)

$S_{34} = \alpha_{3,2,9} + \alpha_{1,2,9}$	C2H bend.
$S_{35} = \alpha_{3,2,9} - \alpha_{1,2,9}$	C2H rock.
$S_{36} = \alpha_{3,2,6} + \alpha_{1,2,6}$	C2C6 bend.
$S_{37} = \alpha_{3,2,6} - \alpha_{1,2,6}$	C2C6 rock.
$S_{38} = 2\alpha_{7,6,8} - \alpha_{2,6,7} - \alpha_{2,6,8}$	COO^- bend.
$S_{39} = \alpha_{2,6,7} - \alpha_{2,6,8}$	COO^- rock.
$S_{40} = 0.653087\alpha_{2,1,5} - 0.505786(\alpha_{1,5,4} + \alpha_{3,2,1}) + 0.175840(\alpha_{5,4,3} + \alpha_{4,3,2})$	Ring bend. I
$S_{41} = 0.404582(\alpha_{3,2,1} - \alpha_{1,4,5}) + 0.579925(\alpha_{5,4,3} - \alpha_{4,3,2})$	Ring bend. II
$S_{42} = 0.615911\tau_{5,4,3,2} + 0.202164(\tau_{2,1,5,4} + \tau_{3,2,1,5}) - 0.519032(\tau_{1,5,4,3} + \tau_{4,3,2,1})$	Ring tors. I
$S_{43} = 0.610119(\tau_{3,2,1,5} - \tau_{2,1,5,4}) + 0.357428(\tau_{1,5,4,3} - \tau_{4,3,2,1})$	Ring tors. II
$S_{44} = \gamma_{7,8,2,6}$	COO^- wagg.
$S_{45} = \tau_{1,2,6,7} + \tau_{1,2,6,8} + \tau_{3,2,6,7} + \tau_{3,2,6,8} + \tau_{9,2,6,7} + \tau_{9,2,6,8}$	COO^- tors.

Table 3. Calculated and experimental frequencies for L-proline and d_2 – L-proline.

Calculated HF/			Experimental			Potential Energy Distribution
6-31G**	6-311G**	6-311++G**	IR	Raman	IINS	(>10%)
68	68	64				$S_{45}(65)$, $S_{43}(33)$
123	123	124	129		134	$S_{43}(43)$, $S_{45}(35)$, $S_{36}(19)$
184	189	187	204		205	$S_{43}(43)$, $S_{37}(30)$
					217	combination
278	287	285	246			$S_{43}(35)$, $S_{39}(26)$, $S_{37}(23)$
307	317	324	295	296	307	$S_{36}(33)$, $S_{42}(31)$
					353	combination
					384	combination
451	451	451	451	450	465	$S_{39}(30)$, $S_{12}(16)$, $S_{13}(11)$, $S_{37}(10)$
551	551	552	573	576	579	$S_{40}(52)$, $S_{29}(19)$
610	612	605				$S_{39}(34)$, $S_{12}(28)$, $S_{14}(13)$
635	636	637	641	641	650	$S_{41}(37)$, $S_{44}(25)$, $S_{39}(11)$
766	771	770	723		709	$S_{44}(33)$, $S_{38}(24)$
807	807	806	791	791	806	$S_{38}(22)$, $S_{44}(14)$
819	817	814				$S_{21}(21)$, $S_{13}(19)$, $S_{25}(14)$, $S_{16}(11)$
832	835	832	847	842	852	$S_{29}(20)$, $S_{33}(13)$, $S_{13}(13)$
864	865	865	860	864		$S_{15}(36)$, $S_{16}(31)$
872	873	872	902	899	884	$S_{17}(18)$, $S_{12}(13)$, $S_{15}(12)$
912	911	910	912	918		$S_{33}(17)$, $S_{15}(13)$, $S_{14}(12)$, $S_{17}(10)$
943	940	942	948	951	934	$S_{21}(39)$, $S_{28}(13)$
996	998	998	980	986	990	$S_{17}(28)$, $S_{16}(18)$
1002	1000	1001	1035	1033		$S_{14}(27)$, $S_{23}(14)$, $S_{35}(12)$
1063	1064	1065	1052	1056	1067	$S_{24}(44)$
1122	1123	1127	1084	1083	1080	$S_{20}(30)$, $S_{34}(28)$
1168	1169	1170	1169	1163		$S_{24}(32)$, $S_{28}(26)$
1198	1206	1213	1179	1175	1194	$S_{19}(33)$, $S_{28}(25)$
1232	1232	1226		1238		$S_{32}(51)$, $S_{35}(21)$
1244	1243	1246	1254			$S_{32}(29)$, $S_{35}(20)$, $S_{19}(14)$
1281	1283	1287		1263		$S_{34}(26)$, $S_{23}(21)$, $S_{20}(15)$
1294	1292	1299	1289	1287		$S_{23}(40)$, $S_{27}(29)$, $S_{19}(11)$
1313	1311	1310	1317	1318		$S_{20}(29)$, $S_{35}(24)$, $S_{10}(14)$
1327	1324	1325				$S_{27}(46)$, $S_{22}(16)$, $S_{35}(15)$
1343	1336	1336	1342	1348		$S_{10}(47)$, $S_{31}(19)$
1371	1369	1367	1377	1374		$S_{31}(46)$, $S_{19}(28)$
1444	1443	1442		1442		$S_{26}(64)$, $S_{22}(27)$
1453	1451	1450	1455	1450		$S_{30}(42)$, $S_{22}(41)$, $S_{26}(11)$
1467	1465	1464		1471		$S_{30}(51)$, $S_{22}(27)$, $S_{26}(17)$
1582	1588	1592	1560	1547		$S_{18}(94)$

Table 3 (continuation)

1768	1747	1718	1621	1622		$S_{11}(90)$
2535	2631	2751				$S_1(89)$
2849	2834	2833	2849			$S_3(98)$
2874	2864	2862	2871	2878		$S_5(98)$
2883	2872	2873		2899		$S_7(96)$
2920	2906	2905	2924	2935		$S_6(88)$
2930	2920	2919	2952	2947		$S_9(97)$
2941	2928	2928		2983		$S_8(84), S_4(11)$
2946	2933	2932		3006		$S_4(87)$
3365	3364	3262				$S_2(100)$
68	67	63				$S_{45}(63), S_{43}(34)$
121	121	121	129		142	$S_{43}(43), S_{45}(37), S_{36}(17)$
183	188	186	206	201	206	$S_4(42), S_{37}(30)$
					221	combination
			246		254	combination
253	265	270	292	294	289	$S_{42}(40), S_{37}(25), S_{39}(24)$
300	303	303	364	354	362	$S_{43}(40), S_{36}(28)$
447	445	446	446	444	455	$S_{39}(32), S_{12}(16), S_{13}(11)$
548	546	547	572	575	554	$S_{40}(49), S_{29}(18)$
603	601	593		609		$S_{39}(28), S_{12}(21)$
614	612	614	634	633	640	$S_{41}(36)$
710	711	710	662	668	663	$S_{21}(55), S_{44}(22)$
760	761	759	768		766	$S_{38}(29), S_{13}(21), S_{44}(13)$
782	781	779	789	789	784	$S_{20}(23), S_{44}(19), S_{17}(13), S_{12}(11)$
816	819	818				$S_{20}(23), S_{17}(19), S_{12}(11)$
835	834	835	829	833		$S_{20}(27), S_{38}(18), S_{13}(11)$
849	847	845	858	861	863	$S_{15}(21), S_{16}(16), S_{33}(16)$
876	874	875	874	879	884	$S_{12}(17), S_{15}(15), S_{21}(14), S_{19}(11)$
898	895	895		897		$S_{25}(24), S_{33}(17), S_{15}(11), S_{20}(11)$
918	916	916	916	920		$S_{20}(23), S_{36}(11), S_{28}(10)$
955	953	956	951	952	942	$S_{16}(28), S_{19}(13), S_{28}(14)$
1014	1011	1014	1015	1014		$S_{14}(25), S_{35}(15), S_{23}(12), S_{15}(10)$
1070	1069	1071	1041	1039	1033	$S_{25}(30), S_{19}(12), S_{33}(10), S_{13}(10)$
1073	1074	1075	1086	1055	1070	$S_{19}(38), S_{28}(12), S_{24}(11), S_{13}(11)$
1152	1151	1155	1124	1104		$S_{19}(44), S_{33}(23), S_{17}(10)$
1167	1164	1165	1161		1141	$S_{24}(29), S_{18}(21), S_{28}(14), S_{35}(11)$
1190	1186	1187	1177	1175		$S_{28}(45), S_{18}(22)$
1243	1239	1241		1238		$S_{31}(59), S_{18}(14)$
1260	1255	1258	1248	1248		$S_{34}(46), S_{24}(21)$
1280	1275	1276	1272	1272		$S_{35}(55)$
1299	1290	1291	1294	1290		$S_{23}(48), S_{27}(21), S_{10}(10)$
1328	1320	1347	1320	1320		$S_{27}(54), S_{10}(13)$
1343	1331	1332	1342	1350		$S_{10}(57), S_{23}(18)$
1352	1347	1347	1381	1381		$S_{31}(73)$
1448	1443	1442		1440		$S_{26}(64), S_{22}(27)$
1457	1451	1450	1451	1450		$S_{22}(43), S_{30}(38), S_{26}(11)$
1473	1466	1466	1480	1473		$S_{30}(55), S_{22}(22), S_{26}(19)$
1757	1735	1708	1602	1618		$S_{11}(85)$
1878	1936	2019	1940	1950		$S_1(82)$
2474	2466	2465	2276	2279		$S_2(96)$
2857	2834	2833	2852			$S_3(98)$
2883	2863	2862	2871	2878		$S_5(98)$
2892	2872	2873		2899		$S_7(96)$
2929	2906	2905	2925	2936		$S_6(88)$
2939	2920	2919	2955	2947		$S_9(97)$
2950	2928	2928	2982	2983		$S_8(84), S_4(11)$
2954	2933	2932	3006	3004		$S_4(87)$

RESULTS AND DISCUSSION

Optimized geometries: Table 1 lists the bond lengths and angles in the zwitterionic form of L-proline molecule calculated using the HF/6-31G**, HF/311G** and HF/6-311++G** levels. All gave the zwitterionic structure. The calculated bond lengths and angles between atoms forming the pyrrolidine ring show reasonable agreement with the experimental data [1]. The pyrrolidine rings in the crystals are in the envelope conformation with the C4 atom 0.60 Å off the mean plane formed by the other atoms. The *cis* orientation of C4 with respect to the carboxylic group is maintained in the optimized structures. In the crystal structure, L-proline molecules form infinite ribbons with the distance of more than 3.5 Å between two nearest atoms, each belonging to the adjacent molecules in the same ribbon. The atoms forming the carboxylic moiety C2–C6–O7–O8 are coplanar with the mean atom deviation from the best plane of 0.006 Å. This group is situated outside the ribbon with the N1–C2–C6 angle of 107.4 deg. All sets reproduce the carboxylic group with the calculated C2–C6 distance longer, the C–O bonds shorter and the O7–C6–O8 angle larger than the respective values observed in experiment (see Table 1). The pyrrolidine nitrogen atom acts as a donor in two hydrogen bonds to the carboxylate oxygen atoms: one of them is formed between the nitrogen atom and the carboxylate oxygen atom belonging to the molecule translated by the unit cell vector c. In this case, the observed N–H...O bond length is 2.69(3) Å and the N–H–O angle 155.6(5) deg. [1]. The other hydrogen bond links the nitrogen atom with the carboxylate oxygen atom of a molecule translated by the unit cell vector b. Its length is 2.71(3) Å and the angle N–H–O 154.4(5) deg. [1]. These bonds are not reproduced in the optimized structure. However, all sets provide an intra molecular hydrogen bond between the pyrrolidine nitrogen atom N1 and the carboxylate oxygen O8 with the lengths ranging from 2.373 to 2.439 Å and the N1–H17–O8 angle between 132.5 and 136.3 deg., depending on the adopted basis set. This strong hydrogen bond was not recognized in [1], but was observed in the crystal structure of L-hydroxyproline determined by neutron diffraction [14].

Vibrational assignments: NH_2^+ group modes. The modes observed on the IINS spectra in the energy transfer range from 100 to 600 cm^{-1} recorded both for normal and deuterated L-proline can be assigned, each to a number of modes but not to the modes related with the vibrations of the NH_2^+ moiety (see Table 3). The modes due to the *rocking* vibrations of the NH_2^+ and the ND_2^+ groups are identified at 994 and 663 cm^{-1}, respectively. However, the first is overlapping with the *twisting* mode of the $C4H_2$ group, the second – with the *wagging* mode of the COO$^-$ moiety. The *twisting* and *wagging* modes of the NH_2^+ group appear at 1008 and 1194 cm^{-1}, while the *wagging* and *bending* modes of the ND_2^+ group can be identified at 1070 and 1141 cm^{-1}, respectively. In the aliphatic amino acids the frequencies assigned to the *out-of-plane* γ(N–H...O) modes related either to intra or intermolecular hydrogen bonds have been observed at the energy transfers less than 600 cm^{-1}, for example at 505 and 513 in L-valine [5], and at 510 and 522 cm^{-1} in L-leucine [6]. Both compounds exhibit the

zwitterionic structure and the triple degenerate torsional vibration of the NH_3^+ moiety is lifted when the hydrogen atoms become engaged in hydrogen bonds. On the other hand, the NH_2^+ moiety in L-proline is a part of a rigid five-membered ring, so that the *bending, wagging, twisting* and *rocking* modes appear at much higher frequencies and are mixed with the modes belonging to other groups. Symmetric and asymmetric *stretching* frequencies of the ND_2^+ group have been identified as single modes at 1940 (IR) and 1950 (Raman) and 2276 (IR) and 2279 cm^{-1} (Raman), respectively. They are not observed on the relevant normal L-proline spectra.

Carboxylic group modes: Asymmetric *stretching* modes of the carboxylic group COO^- in both normal and deuterated L-proline appear as single frequencies at 1621 (IR) and 1622 cm^{-1} (Raman) and at 1602 (IR) and 1618 cm^{-1} (Raman) respectively. The corresponding symmetric *stretching* frequencies for both samples are overlapping with the $C5H_2$ and the $C3D_2$ *wagging* modes. The *bending, wagging* and *rocking* frequencies of normal and deuterated L-proline appear either jointly or are obscured by the modes due to the vibrations of other groups. For example, the frequencies observed on the IR spectrum of normal L-proline at 791 cm^{-1}, at 791 cm^{-1} on the Raman and at 806 cm^{-1} on the IINS patterns were assigned to *bending* and *wagging* modes of the COO^- group only. On the other hand, the frequencies observed on the IR, Raman and IINS spectra at 662, 668 and 663 cm^{-1} of the deuterated sample are assigned to the *wagging* mode of the COO^- moiety and the *bending* mode of the $C2H_2$ group.

CH_2 groups modes: The frequencies contributed by the vibrations of the CH_2 groups are observed in the IINS spectra of both samples in the frequency range from 1000 to 1200 cm^{-1} and up to 1500 cm^{-1} in the IR and Raman spectra. They are assigned to groups of modes, however, only the *twisting* mode of the $C5D_2$ group is represented by a single frequency at 1381 cm^{-1} in the IR and Raman spectra of the deuterated sample.

Pyrrolidine ring modes: The pyrrolidine ring contributes two *in-plane* and two *out-of-plane* frequencies observed in the spectra of both samples in the range from 100 to 660 cm^{-1}. In the spectra of the normal L-proline, these frequencies are overlapping with the other ones contributed, first of all, by the vibrations of the carboxylate group. For example, in the case of normal L-proline the frequency assigned to the ring *in-plane* vibration appears at 641 (IR), 641 (Raman) and 650 cm^{-1} (IINS), but is obscured by the *wagging* and *rocking* frequencies of the COO^- group. On the other hand, this ring *in-plane* mode in the deuterated sample is represented by a single frequency at 634 (IR), 633 (Raman) and 640 cm^{-1} (IINS). A ring *out-of-plane* frequency in the IR and IINS spectra of normal L-proline is observed at 129 and 134 cm^{-1}, respectively, and at 129 (IR) and 142 cm^{-1} (IINS) in the spectra of the deuterated sample. However, for both samples these frequencies can be also assigned to a *wagging* mode of the COO^- group.

CONCLUSIONS

In contrast to aliphatic amino acids, which exhibit the zwitterionic structure, the triple degenerate torsional vibration of the NH_3^+ moiety is lifted when the hydrogen atoms become engaged in hydrogen bonds. The NH_2^+ group in L-proline is a part of a rigid five membered ring and its *bending, wagging, twisting and rocking* modes show much higher frequencies. Consequently, they are overlapping with the frequencies, due to other modes and cannot be uniquely separated and identified by the changes of their positions on the IINS spectra of the normal and deuterated samples.

REFERENCES

1. Kayushina R.I. and Vainshtein B.K., *Kristallogr.*, **10**, 835 (1965).
2. Herlinger A.W. and Long III T.V., *J. Am. Chem. Soc.*, **92**, 77 (1970).
3. Tarakeshwar P. and Manogaran S., *J. Mol. Str. (Theochem)*, **365**, 167 (1996).
4. Tarakeshwar P. and Manogaran S., *J. Mol. Str. (Theochem)*, **417**, 255 (1997).
5. Pawlukojć A., Bobrowicz L., Natkaniec I. and Leciejewicz J., *Spectrochim. Acta*, **A51**, 303 (1995).
6. Pawlukojć A., Leciejewicz J. and Natkaniec I., *Spectrochim. Acta*, **A52**, 29 (1996).
7. Pawlukojć A., Bajdor K., Dobrowolski J.Cz., Leciejewicz J. and Natkaniec I., *Spectrochim. Acta*, **A53**, 927 (1997).
8. Natkaniec I., Bragin S.I., Brankowski J. and Mayer J., Proc. ICANS-XIII, Abbington 1993, RAL Report 94-025, vol. I., p. 89.
9. User Guide. Neutron Experimental Facilities at JINR, Dubna (1992).
10. Frisch M.J.,Trucks G.W., Schlegel H.B., Scuseria G.E, Robb M.A., Cheeseman J.R, Zakrzewski V.G., Montgomery, Jr. J.A., Stratmann R.E., Burant J.C., Dapprich S., Millam J..M., Daniels A.D., Kudin K.N., Strain M.C, Farkas O., Tomasi J., Barone V., Cossi M., Cammi R., Mennucci B., Pomelli C., Adamo C., Clifford S., Ochterski J., Petersson G.A, Ayala P.Y., Cui Q., Morokuma K., Malick D.K., Rabuck A.D., Raghavachari K., Foresman J.B., Cioslowski J., Ortiz J.V., Stefanov B.B., Liu G, Liashenko A., Piskorz P., Komaromi I., Gomperts R., Martin R.L., Fox D.J., Keith T., Al-Laham M.A., Peng C.Y., Nanayakkara A., Gonzalez C., Challacombe M., Gill P.M.W., Johnson B., Chen W., Wong M.W., Andres J.L., Gonzalez C., Head-Gordon M., Replogle E.S., and Pople J.A., Gaussian, Inc., Pittsburgh PA, 1998.
11. Granovsky A.A., http://classic.chem.msu.su/gran/gamess/index.html
12. Schmidt M.W., Baldridge K.K., Boatz J.A., Elbert S.T., Gordon M.S., Jensen J.J., Koseki S., Matsunaga N., Nguyen K.A., Su S., Windus T.L., Dupuis M. and Montgomery J.A., *J. Comput. Chem.*, **14**, 1347 (1993).
13. Kearley G.J., *Nucl. Instrum. Meth.*, **A354**, 53 (1995).
14. Koetzle T.F., Lehmann M.S. and Hamilton W.C., *Acta Cryst.*, **B29**, 231 (1973).